Heterogeneous & Homogeneous & Bio- & Nano-
CHEMCATCHEM
CATALYSIS

Title: SBA-15 Supported Metal Silicides as Efficient Catalysts towards Semihydrogenation of Phenylacetylene by Chemical Vapor Deposition

Authors: Changhai Liang, Kaixuan Yang, Xiao Chen, Lei Wang, Liangliang Zhang, and Shaohua Jin

To be cited as: *ChemCatChem* 10.1002/cctc.201601653

Link to VoR: http://dx.doi.org/10.1002/cctc.201601653

A Journal of
ChemPubSoc Europe

WILEY-VCH www.chemcatchem.org

SBA-15 Supported Metal Silicides as Efficient Catalysts towards Semihydrogenation of Phenylacetylene by Chemical Vapor Deposition

Kaixuan Yang, Xiao Chen, Lei Wang, Liangliang Zhang, Shaohua Jin, and Changhai Liang*

Abstract: The metal silicide (Pd_2Si, Ni_2Si, CoSi, Fe_xSi, and $Cu_{6.69}Si$) catalysts supported by SBA-15 have been successfully prepared by a chemical vapor deposition method at H_2 atmosphere, using $(CH_3)_2SiCl_2$ as the Si source. Compared with those SBA-15 supported metal silicides catalysts, the Ni_2Si/SBA-15 presented modest activity, notable selectivity to styrene (>90 %) and high stability with respect to the selectivity hydrogenation of phenylacetylene, which is attributed to the active-site isolation and electron transfer in silicide. Furthermore, the Ni_2Si/SBA-15 also has high selectivity to diphenylacetylene and 1,4-butynediol, which means that the Ni_2Si/SBA-15 catalyst is a promising low-cost catalysts for succedaneum of noble catalyst as the selectivity hydrogenation catalysts.

Introduction

Liquid-phase selective hydrogenation of carbon-carbon triple bonds is of both industrial and scientific interest, especially phenylacetylene (PA). This compound is an unwanted feedstock component in polystyrene production plants, which would poison the catalysts for styrene (ST) polymerization. Its removal to a level below 10 ppm is mandatory to avoid poisoning of the polymerization catalyst. As shown in scheme 1, the hydrogenation of PA to ethylbenzene (ET) is generally assumed to occur through two consecutive hydrogenation reactions in parallel with a single step that ET can also be directly formed from PA.[1] Therefore, to improve ST yield, not only ST hydrogenated to ET should be minimized, but also the direct hydrogenation of PA to ET should be prevented. Traditionally, Lindlar's catalyst, consisting of Pd poisoned by $Pb(OAc)_2$ and supported on $CaCO_3$, is used as a catalyst to PA hydrogenation.[2] However, a considerable H_2 consumption is noticed over Lindlar's catalyst, due to the overhydrogenation of ST to ET.[3] Moreover, other noble metals catalysts, including supported Pt, Au, and Rh are also used for this reaction, which have been developed and improved over the last few decades.[4] Considering the high cost and sensitivity of noble metals, they are needed to be replaced. In recent years, intermetallic compounds, such as Ni-P, Mo-C, Ni-Ga, and Pd-Ga have emerged as PA hydrogenation catalysts, due to the highly selectivity to ST and the excellent stability.[5]

Recently, metal silicides as new intermetallic compounds have also been used as PA hydrogenation catalysts and shown excellent catalytic performance.[6] However, the preparation of silicides with general and controllable synthesis method is still a big challenge, due to the complex phase behavior between metals and silicon and the complex stoichiometry and structure of their resulting compounds. Chemical vapor deposition (CVD) has been shown to be a powerful method for generating highly dispersed catalysts in a controlled and reproducible manner. Jin et al. have successfully synthesized of CoSi, FeSi, and $MnSi_{1.73}$ nanowires by metal organic chemical vapor deposition using $M(SiCl_3)_x(CO)_y$ (M=Co, Fe, Mn) as a single source precursor.[7] In our previous researches, the supported CoSi, $FeSi_x$, and $MnSi_x$ nanoparticles have been prepared using the same method, which presented high catalytic activity and selectivity in naphthalene hydrogenation.[8] However, the metallic organic precursor is air-sensitive and too expensive, which is not a good candidate to quantity product silicide catalyst.

Therefore, it is necessary to design a general chemical way to the controllable synthesis of metal silicides catalysts. In this work, we reported a general way to prepare SBA-15 supported metal silicides (Pd_2Si, Ni_2Si, CoSi, Fe_xSi, and $Cu_{6.69}Si$ by CVD. The catalytic property of M-Si/SBA-15 has been detected in the semihydrogenation of PA under very mild conditions.

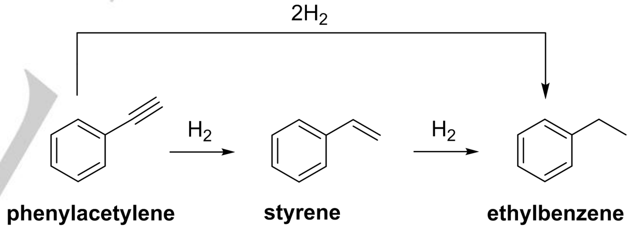

Scheme 1. Reaction network of phenylacetylene hydrogenation

Results and Discussion

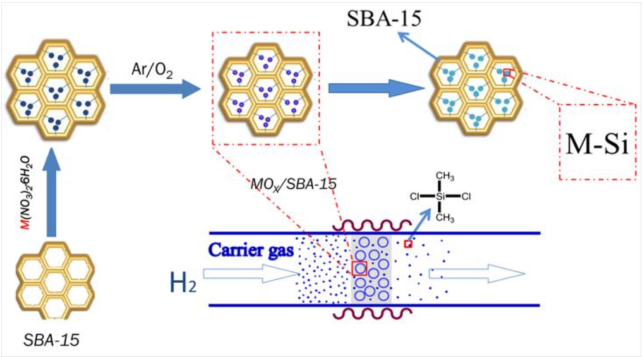

Figure 1. The CVD schematic diagram to prepared M-Si/SBA-15 catalysts.

Kaixuan Yang, Dr. Xiao Chen, Dr. Lei Wang, Shaohua Jin, Prof. Changhai Liang
Laboratory of Advanced Materials and Catalytic Engineering
Dalian University of Technology
116024 Dalian (P. R. China)
E-mail: changhai@dlut.edu.cn

Supporting information for this article is given via a link at the end of the document.

As show in Figure 1, the M-Si/SBA-15 were prepared by the reaction between SBA-15 supported metal nanoparticles and $(CH_3)_2SiCl_2$ in H_2 atmosphere at 600 °C for 2h. The reducing atmosphere (H_2) plays an important role in this process. The Ni_2Si/SBA-15 can be prepared successfully from Ni/SBA-15 at silicification temperature (450 °C) used H_2 as the carrier gas, while the Ni/SBA-15 presented even at 700 °C in Ar (Figure S1). It is reported that metal could catalyze the $SiCl_4$ to generate $SiHCl_3$, SiH_2Cl_2, and even SiH_4 in H_2 atmosphere.[9] The formed SiH_x is easy to react with metal nanoparticles to form metal silicide at relatively low temperature.

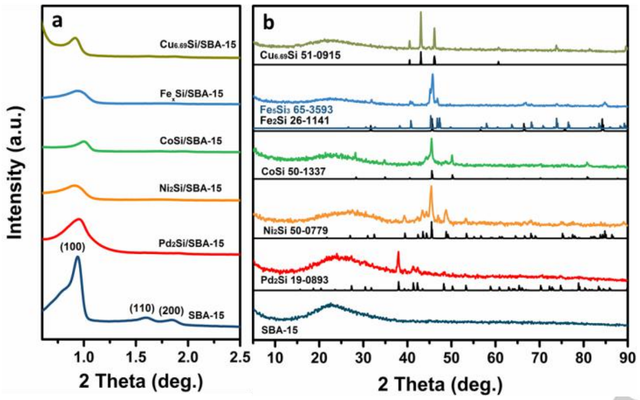

Figure 2. a) Small-angle and b) wide-angel XRD patterns of SBA-15 and SBA-15 supported metal silicides catalysts (SBA-15, Pd_2Si/SBA-15, Ni_2Si/SBA-15, CoSi/SBA-15, Fe_xSi/SBA-15, and $Cu_{6.69}Si$/SBA-15).

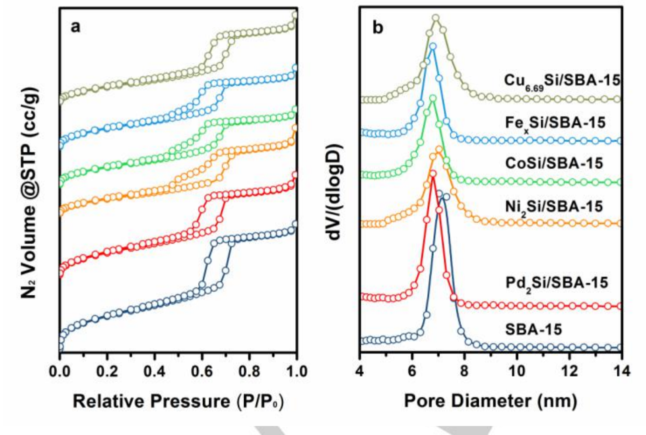

Figure 3. a) Nitrogen adsorption−desorption isotherms and b) BJH pore size distribution of the SBA-15 and M-Si/SBA-15 samples.

The crystal phases of as-prepared M-Si/SBA-15 samples are confirmed by XRD patterns in Figure 2 The small-angle XRD pattern of the SBA-15 (Figure 2a) clearly illustrates three well-resolved diffraction peaks in the small-angle region, which can be indexed as the characteristic (100), (110), and (200) reflections of a two-dimensional hexagonal mesoporous structure. With the formation of M-Si, the (110) and (200) reflections become weak and then disappear, which could be explained by a decrease of the degree of ordering due to the loading of metal silicides nanoparticles into the pore of SBA-15. In the wide-angle region of the XRD patterns (Figure 2b), a broad diffraction peak at ca. 23.4° ascribe to SBA-15 support. Comparing with the standard patterns in Figure 2b, the XRD patterns of M-Si present typical diffraction peaks for the Pd_2Si phase (JCPDS # 19-0893), Ni_2Si phase (JCPDS # 50-0779), CoSi phase (JCPDS # 50-1337), and $Cu_{6.69}Si$ phase (JCPDS # 51-0915), respectively. Moreover, the iron silicide is not a single-phase, which included the Fe_2Si phase (JCPDS # 65-3593) and Fe_5Si_3 (JCPDS # 26-1141). Above all, it is a general way to prepare supported metal silicide catalysts by the CVD method using $(CH_3)_2SiCl_2$ as Si source in H_2 atmosphere.

N_2 adsorption-desorption isotherms were obtained for the calcined mesoporous SBA-15 and M-Si/SBA-15 catalysts as shown in Figure 3 The isotherm of Pd_2Si/SBA-15 catalyst is similar to those of SBA-15 and presents type IV with H1-type hysteresis loop and the capillary condensation step of the hysteresis loop is very steep, which means that the Pd_2Si nanoparticles with 5% loading uniformly disperse on the mesopores in the framework.[10] However, the condensation steps of M-Si/SBA-15 samples ($Cu_{6.69}Si$, Fe_xSi, CoSi, and Ni_2Si) with high loading (20%) become less steep and shift to lower P/P_0 values, indicating the occupancy of some pores by metal silicides in SBA-15 support after the impregnation and silicification. As shown in Table 1, the BET specific surface area of calcined SBA-15 is found to be 757 m^2g^{-1}. The loading of M-Si/SBA-15 decreases the surface area (ca. 350 m^2g^{-1}) and pore volume, which could be due to the confined metal silicides nanoparticles inside and on the SBA-15.

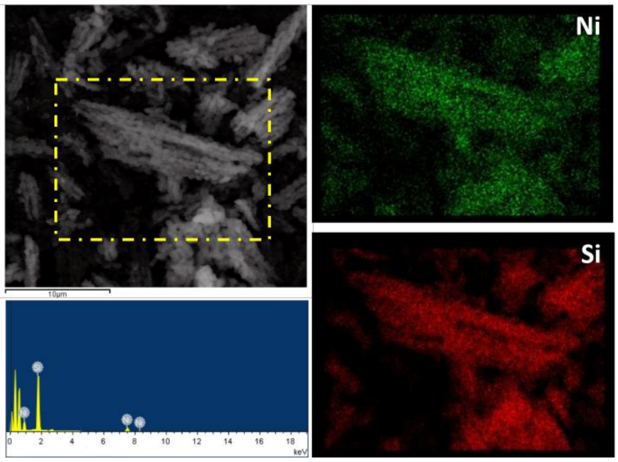

Figure 4. SEM images and Ni-EDX element mapping of Ni_2Si/SBA-15 catalyst.

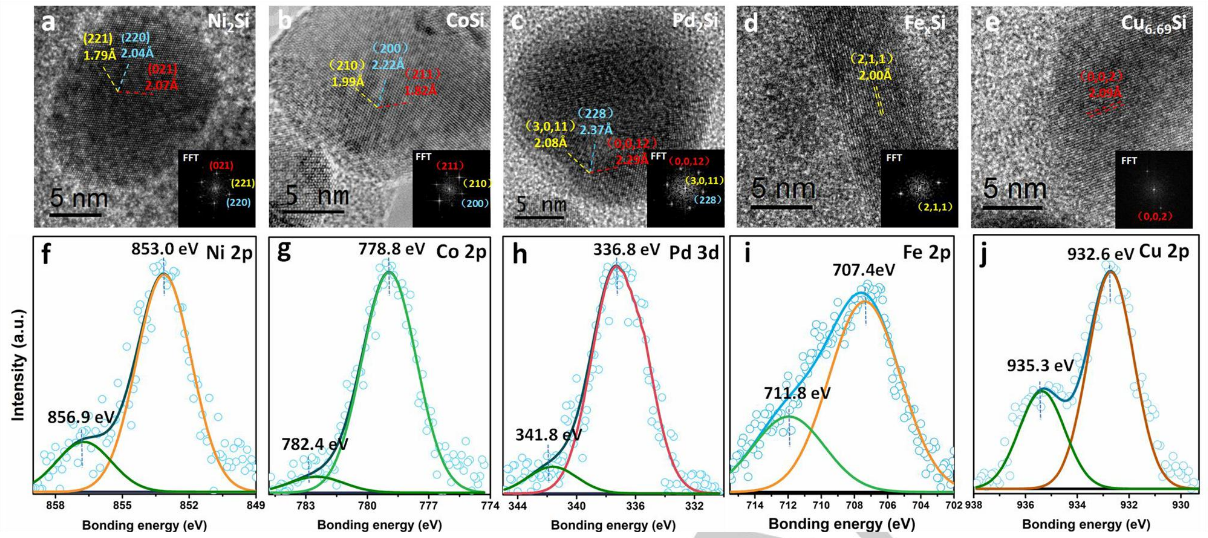

Figure 5. High-resolution TEM images and XPS spectra of (a, f) Ni_2Si/SBA-15, (b, g) CoSi/SBA-15, (c, h) Pd_2Si/SBA-15, (d, i) Fe_xSi/SBA-15, (e, j) $Cu_{6.69}Si$/SBA-15, and their corresponding fast Fourier transformation patterns (inset).

Table 1. Chemical and Structural Properties of SBA-15 supported metal silicide catalysts

Sample	S_{BET}^a (m^2/g)	d^a (nm)	V^a_{total} (cm^3/g)	Metal loadings (wt. %)	
				Reality	Theory
SBA-15	757	7.0	1.002	-	-
Pd_2Si/SBA-15	504	7.0	0.869	4.2	5
Ni_2Si/SBA-15	330	6.8	0.644	18.8	20
CoSi/SBA-15	362	6.8	0.608	17.5	20
Fe_xSi/SBA-15	396	6.8	0.582	17.3	20
$Cu_{6.69}Si$/SBA-15	342	6.8	0.656	18.0	20

^{a}BET surface area (S_{BET}), average pore diameter (d), and total pore volume (V_{total}) as determined by N_2 adsorption−desorption isotherms at −196 °C.

The morphology of Ni_2Si/SBA-15 has been revealed by SEM image (as shown in Figure 4), which consists of rope-like domains with relatively uniform sizes of 1μm and are aggregated into wheat-like macrostructures. And the EDX element mapping confirms that Ni_2Si is highly dispersed throughout all over the SBA-15 support. TEM images provide further insight into the distribution and the detailed structure of metal silicides nanoparticles on SBA-15 in Figure S2 and Figure 5(a-e). The Ni_2Si, CoSi, Pd_2Si, Fe_xSi, and $Cu_{6.69}Si$ nanoparticles are highly dispersed on the SBA-15. The average particle sizes of these catalysts are 14.9 nm, 13.4 nm, 15.6 nm, 16.7 nm, and 14.1 nm, respectively. The high-resolution TEM image (Figure 5a) demonstrates that the measured lattice spacing of nanoparticles are 1.79 Å, 2.04 Å, and 2.08 Å, which are in good accordance with the (221), (220), and (021) planes of orthorhombic Ni_2Si, respectively. Similarly, the measured lattice spacing with 1.99 Å, 2.37 Å, 2.00 Å, and 2.09 Å are corresponding to the (210) plane of Pd_2Si, the (228) plane of CoSi, the (221) plane of Fe_5Si_3, and the (002) plane of $Cu_{6.69}Si$ respectively. The results are similar with that of XRD analysis, which further evidences the formation of metal silicides by the CVD method.

The surface information on the Ni, Co, Pd, Fe, and Cu state are obtained by XPS analysis (Figure 5f-j). The bonding energy peaks of Ni $2p_{3/2}$, Co $2p_{3/2}$, and Pd $3d_{5/2}$ at 853.0 eV, 778.8 eV, 336.8 eV are responding to Ni_2Si, CoSi, and Pd_2Si, respectively.[11] The peak at 707.4 eV for Fe-sample belongs to Fe-Si.[12] The second peaks of Ni 2p and Co 2p at 856.9 and 782.4 eV are assigned to less-intense asymmetric tail for the nickel silicide and cobalt silicide.[11b, 13] And the peak at 341.8 eV belongs to the Pd $3d_{3/2}$ of Pd_2Si.[11c] The peak at 711.5 eV in Figure 5i is analogously attributed to Fe_2O_3.[14] The Cu $2p_{3/2}$ spectrum in Figure 5j appears as narrow doublet peaks at 935.3 eV and 932.6 eV. The peak at 932.6 eV has rarely been reported so far. However, because of evidence from the XRD and HRTEM, it is possible to assign the peak at 932.6 eV to a single compound of copper silicide ($Cu_{6.69}Si$). Compared with the zero valent metal, the peak of metal silicides shifts to higher binding energy, which can be attributed to the electron transformation between metal atoms and Si atoms.

To confirm the catalytic performance over the as-obtained M-Si/SBA-15 catalysts in liquid-phase PA selective hydrogenation, the reaction was carried out at 40 °C and 1.0 MPa H_2 in a conventional batch system. The plots of the ST selectivity versus PA conversion over the metal silicides catalysts are shown in Figure 6a. Unfortunately, the selectivity to ST over Pd_2Si/SBA-15 dramatically decreases with increasing the conversion of PA. The selectivity to ST is only 13% when the PA is completely consumed. This is probably due to the high Pd loading in the Pd_2Si/SBA-15, which would result in higher H_2 activation under reaction condition. Although the CoSi/SBA-15,

10.1002/cctc.201601653

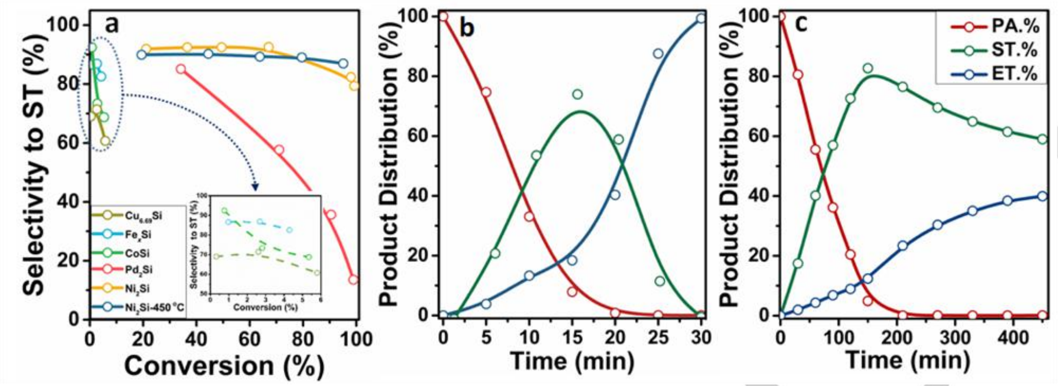

Figure 6. a) The catalytic conversion of PA and corresponding selectivity to ST over different catalysts and the reaction detail of CoSi/SBA-15, Fe_xSi/SBA-15, an $Cu_{6.69}Si$ /SBA-15(inset). Product yields over b) Ni/SBA-15 and c) Ni_2Si-450 °C/SBA-15. (The reaction was carried out at 40 °C, 1.0 MPa H_2 with 100 mg catalyst.)

Fe_xSi/SBA-15, and $Cu_{6.69}Si$/SBA-15 catalysts present good ST selectivity of ca.74%, ca.88%, and ca.72%, respectively, they have low activity to hydrogenate of PA. The whole product yield is even lower than 6% for 6 h. Compared to those catalysts, the Ni_2Si/SBA-15 catalyst has the best performance to selectivity hydrogenation of PA. As observed, high ST selectivity (around 90%) is achieved before the complete conversion of PA for the Ni_2Si/SBA-15 catalyst. As shown in Figure 6a, for the semihydrogenation of PA over Ni_2Si/SBA-15, the selectivity to ST is 82% when the PA conversion reaches to 98%. Fortunately, the selectivity to ST is still at ca. 80% when the PA is almost consumed completely (PA conversion 99%). Therefore, the Ni_2Si/SBA-15 catalyst is a promising low-cost catalyst for succedaneum of noble catalyst to semihydrogenation of PA. Figure S3 shows the result of H_2-TPD measurements over these catalysts. There is almost no H_2 adsorption over CoSi/SBA-15, Fe_xSi/SBA-15, and $Cu_{6.69}Si$/SBA-15 in Figure S3. It is in keeping with that CoSi/SBA-15, Fe_xSi/SBA-15, and $Cu_{6.69}Si$/SBA-15 have the worst activity in the semihydrogenation of PA. Pd_2Si/SBA-15 has best ability to H_2 activation which causes the excessive hydrogenation. Ni_2Si/SBA-15 has the best selectivity to ST because of the proper H_2 activation. Moreover, a stronger electronic interaction between the metallic Ni and the Si may influence the ST adsorption and reduced the reaction rates of ST hydrogenation. Therefore, the Ni_2Si/SBA-15 catalyst is a promising low-cost catalyst for succedaneum of noble catalyst to semihydrogenation of PA. In addition, the synthesis temperature effect on catalytic performance was also tested (as shown in Figure 6a and Figure S4). Compared with Ni_2Si/SBA-15 prepared at 600 °C, the Ni_2Si/SBA-15 prepared at 450 °C shows a better catalytic performance. The selectivity to ST over Ni_2Si-450 °C/SBA-15 catalyst is ca. 90%, while the activity is better (Figure S4), due to the particle size affection.[5b]

The time course of the product yields over and Ni/SBA-15 and Ni_2Si/SBA-15 (prepared at 450 °C) catalysts are shown in Figure 6b and 6c. The reaction rate over Ni_2Si/SBA-15 catalyst from ST to ET is 4.6×10^{-4} mol L^{-1} min^{-1}, which is much lower than the reaction rate from PA to ST (3.0×10^{-3} mol L^{-1} min^{-1}). This indicates that the Ni_2Si/SBA-15 catalyst has high selectivity to ST. However, the reaction rate over Ni/SBA-15 catalyst from PA to ST is almost equal to the rate from ST to ET, which means Ni/SBA-15 catalyst has no selectivity hydrogenation property in this reaction. In our previous available studies, it is found that the silicide-modified nickel catalysts have lower intrinsic activity than the sample Ni because active-site (Ni) is isolated by interposition of Si element. Moreover, there is electron transformation between Ni atom and Si atom, due to the different electronegativity values of Ni (1.91) and Si (1.90).[6a This phenomenon is similar to Ni-Ga intermetallic compounds.[15 Therefore, the active-site isolation and electron transfer in Ni_2Si have a great effect on the performance of PA semihydrogenation to ST. The formation of nickel silicides decreases the adsorption of ST and H_2, thus inhibits the deep hydrogenation of styrene hydrogenation and improves the selectivity to ST.

The stability of Ni_2Si/SBA-15 (prepared at 450 °C) catalyst was investigated by recycling for five times. The conversion of PA and corresponding selectivity toward ST over Ni_2Si/SBA-15 catalyst are shown in Figure 7. The selectivity to ST still keeps almost constant at 90%, and a slight decrease in conversion is found (from 83.2% to 71.5%) after 5 recycles. The decrease of conversion may ascribe to the agglomeration of Ni_2Si particles in the recycle. Moreover, the active sites covered by the strong adsorbed species may be another reason, which could be recovered by removing the strong adsorbed species at higher temperature. Compared with our previous report, the SBA-15 supported Ni_2Si nanoparticles catalyst show a satisfactory stability and reusability than that of bulk silicide modified nickel catalysts.[6a] The spent Ni_2Si catalyst was characterized by XRD, TEM, and XPS (as shown in Figure 8). Compared Figure 2 with Figure 8, no obvious change was observed in the XRD patterns, except that the crystallinity of Ni catalyst increased slightly. The XRD pattern of used catalyst still present typical diffraction peaks of Ni_2Si phase (JCPDS # 50-0779). The TEM image of used catalyst shows a good dispersion. The estimated average particle size of the used catalysts calculated by Scherrer's equation is 12.2 nm, which is a bitter bigger than the fresh catalyst (10.8 nm). The binding energy peak of Ni $2p_{3/2}$ at 853.0

eV is corresponding to Ni_2Si and the peak at 857.3 eV belongs to the less-intense asymmetric tail of Ni_2Si.[11a] All those results demonstrate that the Ni_2Si/SBA-15 catalyst is thermal and electronically stable during the process of PA semihydrogenation. Therefore, the Ni_2Si/SBA-15 shows a better stability in the PA semihydrogenation. The selective hydrogenation of diphenylacetylene and 1,4-butynediol over Ni_2Si/SBA-15 has been further studied, as listed in Table 2. The Ni_2Si/SBA-15 also shows high selectivity (>85%) to the semihydrogenation product and acceptable activity. The above features suggest that Ni_2Si/SBA-15 is a legitimate alternative to non-precious metal catalysts in selective hydrogenation reactions. The unique structural feature of metal silicide may impose effects on catalytic performance.

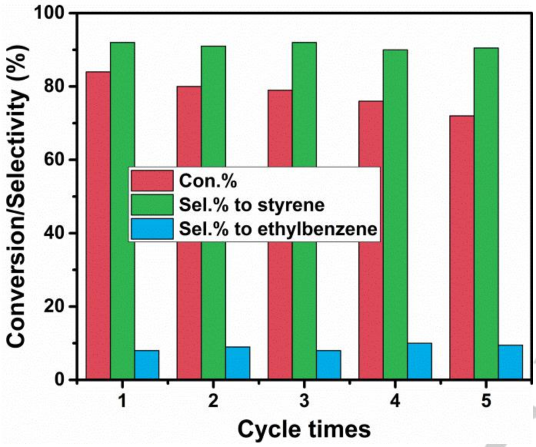

Figure 7. The catalytic conversion and corresponding selectivity vs recycling times over Ni_2Si/SBA-15 catalyst without adding new catalysts. (The reaction was carried out at 40 °C and 1.0 MPa H_2 in 2 h)

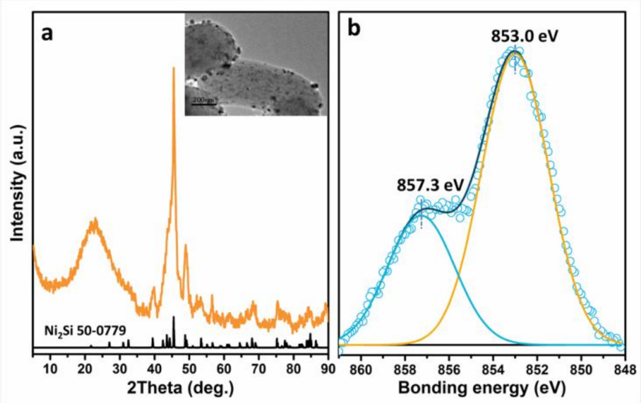

Figure 8. (a) XRD pattern, (inset in a) TEM image, and (b) XPS spectrum of the spent Ni_2Si/SBA-15 catalyst.

Table 2. The catalytic performances of Ni_2Si/SBA-15: selective hydrogenation of phenylacetylene, diphenylacetylene, and 1,4-butynediol

Reactant	Conversion[a] %	Selectivity[a] %
phenylacetylene	81.5	91.5
diphenylacetylene	19.5	92.3
1,4-butynediol	75.3	85.2

[a] The reaction was carried out at 40 °C and 1.0 MPa H_2 in 2 h.

Conclusions

In summary, it is a general method to prepare the metal silicide catalysts supported on SBA-15 (such as Ni_2Si, Pd_2Si, CoSi, $Cu_{6.69}Si$, and Fe_xSi) by the CVD, using $(CH_3)_2SiCl_2$ as Si source. Among those catalysts, the Ni_2Si/SBA-15 has the superior catalytic performance in selectivity hydrogenation of PA to ST. The maximum yield to ST with Ni_2Si/SBA-15 catalyst is higher than with Ni/SBA-15 (83% vs 73%). The formation of nickel silicides influenced the styrene adsorption and reduced the reaction rates of styrene hydrogenation because of the active-site isolation and electron transfer. Therefore, the Ni_2Si/SBA-15 catalyst is a promising low-cost selective hydrogenation catalyst for alternative of noble catalyst.

Experimental Section

Materials. Metal nitrate ($Pd(NO_3)_2$, $Ni(NO_3)_2$, $Co(NO_3)_2$, $Cu(NO_3)_2$, and $Fe(NO_3)_3$), pure ethanol, and hydrochloric acid were obtained from Sinopharm (Beijing, China). Dichlorodimethylsilane, phenylacetylene, diphenylacetylene, 1,4-butynediol, and P_{123} were obtained from Aladdin (Shanghai, China). All of these chemicals were used as received without further purification.

Synthesis of M-O/SBA-15 precursor. SBA-15 was produced by following the same procedure as Zhao's research.[10a] The M-O/SBA-15 precursor was prepared by impregnating the SBA-15 in an aqueous solution of metal nitrate and held for 24 h. Following the soaking, the soaked samples were dried and calcinated in Ar/O_2 atmosphere at 400 °C for three hours. The $Pd(NO_3)_2$, $Ni(NO_3)_2$, $Co(NO_3)_2$, $Fe(NO_3)_3$, and $Cu(NO_3)_2$ were used as metal source and the loading with SBA-15 carrier was 20%, except the 5% loading of $Pd(NO_3)_2$.

Synthesis of M-Si/SBA-15 catalysts. Synthesis of M-Si/SBA-15 was achieved in a horizontal tube furnace at the relevant temperature and atmospheric pressure. The M-O/SBA-15 samples were loaded on a quartz boat and put in the middle of a quartz tube furnace. The M-O/SBA-15 samples were heated at a ramp rate of 5 °C/min to 400-500 °C and held for 2 hours to reduce the M-O to metal. When the furnace temperature was increased to setting temperature, the organosilane was introduced to the reactor by using H_2 (30 sccm) as the carrier gas that flows through a bubbler maintained at 0 °C containing $(CH_3)_2SiCl_2$ and the exhaust was absorbed by 2 mol/L NaOH solution. After 2 h, the product was cooled down to the room temperature in Ar and passivated in Ar overnight.

Catalysts Characterization. X–ray diffraction (XRD) analyses of the samples were carried out using a Rigaku D/Max–RB diffractometer with a Cu Kα_1 monochromatized radiation source, operated at 40 kV and 100 mA. Analysis of element contents of M-Si catalysts was carried out on an Inductively Coupled Plasma Optical Emission Spectrometer (ICP–OES). Nitrogen adsorption and desorption isotherms were constructed using the multi–point method at –196 °C, and were measured using a Micrometrics

2020. The morphology and structural composition of Ni_2Si/SBA-15 sample were characterized and analyzed by high-resolution field emission scanning electron microscopy (FE–SEM, Nova NanoSEM 450 from FEI Company), equipped with an energy–dispersive X–ray (EDX) analyzer. Transmission electron microscopy (TEM) and were performed by using a Tecnai G2 F30 S–Twin transmission electron microscope operating at 300 kV. Surface compositions were investigated by X–Ray photoelectron spectroscopy (XPS) employing an ESCALAB250 (Thermo VG, USA) spectrometer with Al Kα (1486.6 eV) radiation with a power of 150 W. All core–level spectra were referenced as the C 1s neutral carbon peak at 284.6 eV and were deconvoluted into Gaussian component peaks.

M-Si/SBA-15 catalysts test. According to the procedure previously employed,[6a] PA hydrogenation (Scheme 1) were performed with metal silicide catalysts in a 50 mL stainless steel autoclave under vigorous stirring. Before reaction, catalysts were activated in an ultrapure hydrogen stream at 400 °C for 2 h and then cooled down to room temperature and passivated in Ar for 12 h. The reaction was carried out at 40 ^{o}C temperature and 1 MPa H_2 with 0.10 g catalyst in 10 mL 0.1 M ethanol substrate solution. The products were analyzed by gas chromatography using a flame ionization detector with a SE-54/52 capillary column. A known amount of n-octane solution was used as an internal standard in this analysis. The stability of Ni_2Si-450/SBA-15, is also tested at 40 ^{o}C and 1 MPa H_2 for 5 times.

Acknowledgements

We gratefully acknowledge the financial support provided by the National Natural Science Foundation of China (21373038 and 21403026), the China Postdoctoral Science Foundation (2015T80255), the Natural Science Foundation of Liaoning Province in China (2015021014) and Program for Excellent Talents in Dalian City (2016RD09).

Keywords: Metal Silicide • Chemical vapor deposition • Phenylacetylene Hydrogenation

[1] B. A. Wilhite, a. M. J. McCready, A. Varma, *Ind. Eng. Chem. Res.* **2002**, 3345-3350.
[2] H. Lindlar, Helv. *Chim. Acta* **1952**, 35, 446–450.
[3] H. Lindlar, R. Dubuis, Organic Syntheses. John Wiley & Sons, Inc. **2003**, 89-89.
[4] a) C. Li, Z. Shao, M. Pang, C. T. Williams, C. Liang, *Catal. Today* **2012**, 186, 69-75; b) T. Lopez, R. Gomez, E. Romero, I. Schifter, React. Kinet. *Catal. Lett.* **1993**, 49, 95-101; c) X. Y. Quek, Y. Guan, R. A. Santen van, E. Hensen, X. Y. Quek, Y. Guan, R. A. Santen van, E. Hensen, *ChemSusChem* **2010**; d) L. Shao, X. Huang, D. Teschner, W. Zhang, *ACS Catal.* **2014**, 4, 2369-2373.
[5] a) Y. Chen, C. Li, J. Zhou, S. Zhang, D. Rao, S. He, M. Wei, D. G. Evans, X. Duan, *J. Exp. Zool.* **2015**, 5, 5756-5765; b) C. Li, Y. Chen, S. Zhang, J. Zhou, F. Wang, S. He, M. Wei, D. G. Evans, X. Duan, *ChemCatChem* **2014**, 6, 824–831; c) M. Pang, Z. Shao, W. Xia, X. Wang, C. Liang, *AIChE J.* **2015**, 61, 2522-2531; d) G. Wowsnick, D. Teschner, M. Armbrüster, I. Kasatkin, F. Girgsdies, Y. Grin, R. Schlögl, M. Behrens, *J. Catal.* **2014**, 309, 221–230.
[6] a) X. Chen, A. Zhao, Z. Shao, C. Li, C. T. Williams, C. Liang, *J. Phys Chem. C* **2010**, 114, 16525-16533; b) K. Yang, C. Xiao, J. Guan, C. Liang *Catal. Today* **2014**, 246, 176–183.
[7] a) S. N. Girard, X. Chen, F. Meng, A. Pokhrel, J. Zhou, L. Shi, S. Jin, *Chen Mater.* **2014**, 26, 5097-5104; b) A. L. Schmitt, Z. Lei, D. Schmeisser, F. J Himpsel, J. Song, *Cheminform* **2006**, 110, 18142-18146; c) J. R. Szczech, *J Mater. Chem.* **2010**, 7, 1375-1382.
[8] a) J. Guan, J. Jin, X. Chen, B. Zhang, D. Su, C. Liang, *Chem. Vap Deposition* **2013**, 19, 68-73; b) J. Guan, A. Zhao, X. Chen, M. Zhang, C. Liang *Stud. Surf. Sci. Catal.* **2010**, 175, 259-262; c) A. Zhao, X. Zhang, X. Chen, J Guan, C. Liang, *J. Phys. Chem. C* **2010**, 114, 3962-3967.
[9] a) H. Walter, G. Roewer, K. Bohmhammel, *J.chem.soc.faraday Trans* **199** 92, 4605-4608; b) K. Bohmhammel, G. Roewer, H. Walter *J.chem.soc.faraday Trans* **1995**, 91, 3879-3882; c) P. Li, T. Wang, *Chin. J Chem. Eng.* **2015**, 23, 681-688.
[10] a) D. Zhao, J. Feng, Q. Huo, N. Melosh, G. H. Fredrickson, B. F. Chmelk G. D. Stucky, *Science* **1998**, 279, 548-552; b) D. Zhao, J. Sun, Q. Li, G. D Stucky, *Chem. Mater.* **2000**, 12, 275-279.
[11] a) S. A Pérez - García, L. Nyborg, *Surf. Interface Anal.* **2006**, 38, 859-86 b) J. Zhao, D. M. Poirier, *Surf. Sci. Spectra* **2000**, 329; c) P. J. Grunthaner, F J. Grunthaner, A. Madhukar, *J. Vac. Sci. Technol.* **1982**, 20, 680-683.
[12] I. N. Shabanova, V. A. Trapeznikov, *J. Electron Spectrosc. Relat Phenom.*, **1975**, 6(4):297-307.
[13] M. GarcíA-Méndez, F. F. Castillón, G. A. Hirata, M. H. FaríAs, G Beamson, *Appl. Surf. Sci.* **2000**, 161, 61-73.
[14] D. W. Oscarson, P. M. Huang, C. Defoss, A. Herbillion, *Nature*, **1981**, 291
[15] a) L. S. Hsu, A. I. Nesvizhskii, *J. Appl. Phys*. **2002**, 62, 1103-1109; b) Y Liu, X. Liu, Q. Feng, D. He, L. Zhang, C. Lian, R. Shen, G. Zhao, Y. Ji, D Wang, *Adv. Mater*. **2016**, 28, 4747-4754.

FULL PAPER

The metal silicide (Pd_2Si, Ni_2Si, CoSi, Fe_xSi, and $Cu_{6.69}Si$) catalysts supported by SBA-15 are successfully prepared by chemical vapor deposition method. Compared with those SBA-15 supported metal silicides catalysts, the Ni_2Si/SBA-15 presented modest activity, notable selectivity to styrene (>90 %) and highly stability in the selectivity hydrogenation of phenylacetylene.

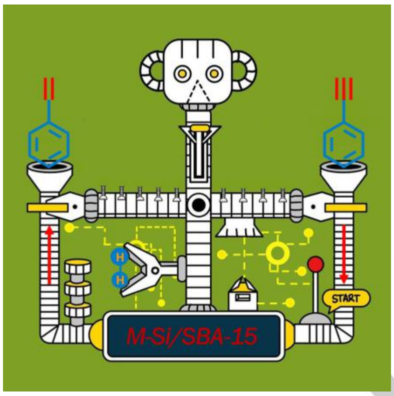

*Kaixuan Yang, Xiao Chen, Lei Wang, Liangliang Zhang, Shaohua Jin, Changhai Liang**

Page No. – Page No.

SBA-15 Supported Metal Silicides as Efficient Catalysts towards Semihydrogenation of Phenylacetylene by Chemical Vapor Deposition